

Search for anomalous neutral current coherent-like single-photon production in MicroBooNE

The MicroBooNE Collaboration*

May 26, 2022

Abstract

MicroBooNE is a liquid argon time projection chamber (TPC) detector which offers excellent spatial and energy resolution and the ability to distinguish electrons from photons. In this note we present preliminary results from a dedicated search for neutral current (NC) single-photon production, with a focus on forward-going photons and no visible hadronic activity, both of which are key characteristics of “coherent-like” electromagnetic shower production. A total efficiency for SM-predicted NC coherent 1γ events of 12.5% is obtained, defined relative to simulated events in the entire MicroBooNE active TPC. Relative to the Pandora-reconstructed single-shower event selection, the analysis achieves a 95% rejection of non-coherent NC $1\pi^0$ background events and a 99.97% rejection of cosmic background events, while maintaining a signal efficiency of approximately 45%.

*Email: microboone_info@fnal.gov

Contents

1	Introduction	3
2	Analysis Description	3
2.1	Signal and Background Simulation	3
2.2	Event Breakdown	4
2.3	Analysis Flow	5
2.4	Preliminary Results on Simulation	8
2.5	Potential Future Improvements	9
3	Summary	14

1 Introduction

The MicroBooNE experiment is a liquid argon time projection chamber (LArTPC) situated on-axis of the Booster Neutrino Beam (BNB), 468 meters downstream from the BNB target [1]. The experiment has recently completed its operations, collecting neutrino interaction data corresponding to a beam delivery of $\sim 1.2 \times 10^{21}$ protons on target (POT), over Runs 1-5 during 2015-2020.

One of the main physics goals of MicroBooNE is to investigate the anomalous low-energy excess (LEE) observed by MiniBooNE [2] under two hypotheses: the excess consists of photons or electrons. MicroBooNE published its first search for a photon excess in October 2021 [3], where it excluded the interpretation of the LEE as a 3.18 times enhancement of the Standard Model (SM) process NC Δ radiative decay rate [4] at 1.9σ , in favor of its nominal rate. The analysis presented in this note builds upon one of the exclusive topological selections ($1\gamma 0p$) of [3], which consisted of a single (1) shower and zero (0) tracks, with focus on optimizing sensitivity to a single-photon-like final state which is produced in the forward (neutrino beam) direction. The signal used to develop this analysis is neutrino NC coherent single-photon production on argon, which is modeled in [5]. While the SM-predicted rate for NC coherent single-photon production is beyond the sensitivity reach of the MicroBooNE experiment, this process has never before been measured, and this search represents an opportunity to produce a world-leading limit with sensitivity to an anomalously large NC coherent single-photon-like rate. The latter is theoretically motivated by models of coherent-like e^+e^- production, such as [6, 7, 8, 9], which are capable of producing pairs of e^+e^- that completely overlap and thus can explain the MiniBooNE LEE.

The analysis presented in this note is being developed as a blind analysis, and the selection has been developed and optimized using only MicroBooNE Runs 1-3 Monte Carlo simulation, corresponding to a BNB exposure of 6.8×10^{20} POT.

2 Analysis Description

The MicroBooNE NC coherent-like single-photon search analysis begins with events that consist of only one shower reconstructed by Pandora [10], and subsequently pre-selection cuts are applied to ensure well-reconstructed events and remove clear background topologies. Then, a series of carefully designed boosted decision tree (BDT) selections, each targeting a specific dominant background, is applied. The analysis approach is built upon the successful MicroBooNE NC Δ radiative decay search analysis [3], with improved non-photon background rejection. This section first describes signal and background simulation in Sec. 2.1 and breakdown of different background events in Sec. 2.2, followed by a more detailed description of the analysis flow in subsequent Sec. 2.3, and preliminary results in Sec. 2.4. Future improvement to reject events with visible (and often non-reconstructed) hadronic vertex activity, via use of a new analysis tool - the Proton Stub Veto (PSV) - is discussed in detail in Sec. 2.5.

2.1 Signal and Background Simulation

The theoretical model for NC coherent 1γ signal is the photon emission model of L. Alvarez-Ruso *et al.* [5]. This model is not yet included in the neutrino event generator (GENIE v3.0.6) adopted by MicroBooNE but has been implemented in the upcoming, updated GENIE version that is used to simulate signal events in this analysis. Figure 1 shows area-normalized truth level distributions of the simulated NC coherent 1γ photons highlighting the energy range and forward nature of photons that this analysis targets. The NC coherent 1γ model implemented in GENIE

has a built-in cutoff in photon energy of 140 MeV, to avoid dealing with infrared divergence when the photon energy approaches zero. This value corresponds to MiniBooNE’s visible energy cut [5, 11], as the model was initially developed in parallel with studies of the MiniBooNE LEE.

After GENIE simulation, dedicated data collected when the neutrino beam is off (referred to as “BNB-external” data) are overlaid to the signal events to simulate surrounding cosmic background interactions. Then, events are passed to GEANT4, which simulates interactions of final state particles as they propagate through the liquid argon volume, followed by detector response simulation and reconstruction (GEANT4 and detector response simulation only apply to the simulated signal).

Approximately 250,000 coherent single-photon signal events were simulated and reconstructed for this analysis. The estimated number of NC coherent 1γ events expected in the MicroBooNE active detector volume is 12 for Run 1-3 data, assuming that the overall NC coherent 1γ rate is one tenth (1/10) of the overall NC Δ radiative decay rate. This assumption is consistent with the ratio of coherent to NC Δ single-photon production cross sections at the neutrino energy of 600 MeV.

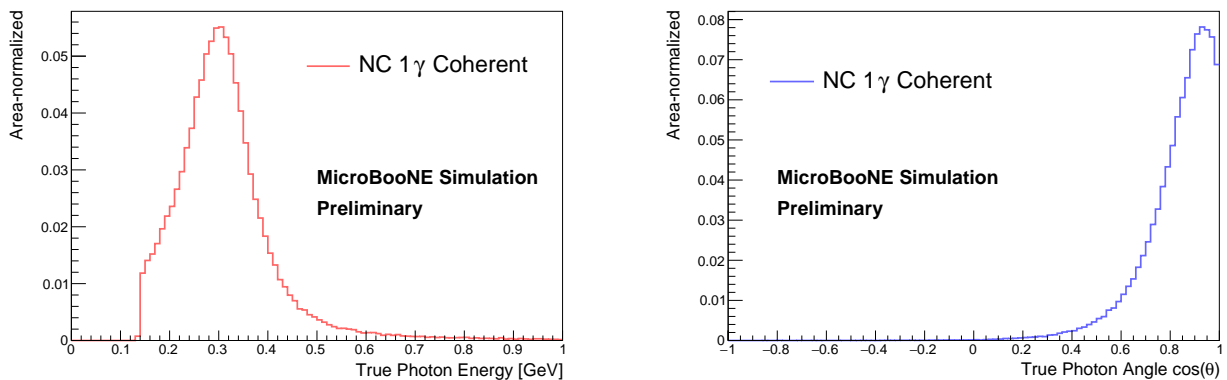


Figure 1: Area-normalized distribution of true energy and angle with respect to the beam direction of simulated NC 1γ coherent events. Note the 140 MeV cutoff introduced to avoid a divergence in the modeling.

Background neutrino-argon interactions are simulated using a custom tune [12] of the GENIE v3.0.6 [13, 14] adopted by the MicroBooNE Collaboration. Similar to the signal simulation, different BNB-external data samples are overlaid to Monte Carlo events for a more realistic simulation. Misidentified cosmic background is estimated separately by real data collected when the neutrino beam is off.

2.2 Event Breakdown

The NC coherent 1γ signal includes any true NC coherent 1γ events with true interaction vertex inside MicroBooNE active TPC volume. The background is divided into different categories according to the truth information and listed below:

- **NC Δ radiative 1(+) protons:** True NC Δ radiative events with true interaction vertex inside the active TPC and at least one proton exiting the nucleus with kinetic energy (KE) larger than 50 MeV, which is the threshold for protons to be generally “reconstructable” in Pandora.
- **NC Δ radiative 0 proton:** A complement of the NC Δ radiative 1(+) protons set. This category includes both NC $\Delta \rightarrow n + \gamma$ and NC $\Delta \rightarrow p + \gamma$ events which have low KE (<50 MeV) protons exiting the nucleus. These low KE protons are considered undetected in our analysis because of low Pandora reconstruction efficiency for them.

- **NC $1\pi^0$** : True NC events with exactly one final-state π^0 with true interaction vertex inside the active TPC. We further split this category into coherent (**NC $1\pi^0$ Coherent**) and non-coherent (**NC $1\pi^0$ Non-Coherent**) events.
- **CC $\nu_\mu 1\pi^0$** : True charged current (CC) ν_μ events with exactly one final-state π^0 with true interaction vertex inside the active TPC. This does not include $\bar{\nu}_\mu$ interactions.
- **CC $\nu_e/\bar{\nu}_e$** : True CC ν_e or $\bar{\nu}_e$ events with true interaction vertex inside the active TPC.
- **BNB Other**: All neutrino-induced events that do not fall into any of the above categories with true interaction vertex inside the active TPC. This category includes NC $\bar{\nu}_\mu$ interactions that are not covered by other categories and any CC $\bar{\nu}_\mu$ interactions.
- **Dirt (Outside TPC)**: All neutrino-induced events that occur externally to the active TPC but deposit energy inside the active TPC volume.
- **Cosmic data**: The cosmic background events are taken directly from MicroBooNE BNB-external cosmic data instead of Monte Carlo simulations for a more realistic and accurate evaluation.

2.3 Analysis Flow

The event selection can be divided into three steps: First is topological selection, where we require exactly 1 reconstructed shower and 0 reconstructed tracks after Pandora reconstruction. Second is pre-selection, where we apply cuts on shower start containment (the shower start point must be greater than 2 cm away from the space-charge [15] boundary of the TPC) and shower energy (shower energy must be greater than 50 MeV) to remove any badly reconstructed events or background events that can be easily removed. Figure 2 shows the reconstructed shower energy distribution after each stage and highlights different types of dominant backgrounds at pre-selection stage: cosmic, Dirt, BNB Other, NC non-coherent $1\pi^0$ and CC ν_μ events, ordered in decreasing number of events. To remove as much of these backgrounds while retaining a high signal selection efficiency given the rareness of the signal, BDTs with XGBoost algorithms [16] are explored. Optimizing and applying cuts on BDT scores comprise the third analysis step and the final selection stage.

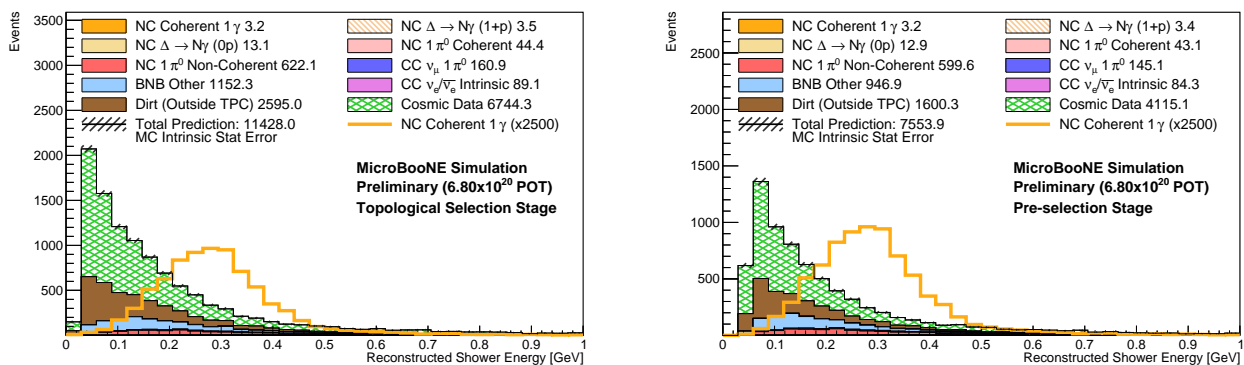


Figure 2: Reconstructed shower energy distribution after topological cuts (left) and pre-selection cuts (right) are applied. Only statistical error is shown in these plots. Note the rarity of the coherent 1γ samples with only 3.2 events for the full $6.8e20$ POT, with over 7,500 background events expected at pre-selection stage. The orange histogram overlaid is the distribution of NC coherent 1γ signal scaled by a factor of 2500 for it to be visible.

BDTs	Goal	Handles
NC π^0	Remove NC $1\pi^0$ background, which is the hardest background to remove	Photon from π^0 decay is less forward going and will have higher momentum projected perpendicular to neutrino beam direction.
Second Shower Veto (SSV)	Identify any candidate activity from missed second shower from π^0 decay in NC $1\pi^0$ events. Output of SSV is fed into NC π^0 BDT as training variables	Assuming the reconstructed shower is truly a shower from π^0 decay, the true second shower from π^0 decay is generally close to the interaction vertex, and the invariant mass it forms with the reconstructed shower is close to the true π^0 mass
Cosmic	Reject cosmic background	Utilizes the fact that a majority of cosmic backgrounds are mis-identified muons and mostly coming from the top of the detector downwards
CC ν_e	Reject mis-identified true CC $\nu_e/\bar{\nu}_e$, improve photon purity of selection	Difference in average deposited energy per length (dE/dx) at the shower start between electromagnetic (EM) shower from photons and EM shower from electrons
CC ν_μ focused	Remove any backgrounds other than cosmic, NC Δ radiative, CC $\nu_e/\bar{\nu}_e$ or NC $1\pi^0$, mostly CC $\nu_\mu/\bar{\nu}_\mu$ background	Muons are minimum-ionizing-particles (MIPs) thus dE/dx at the shower start for mis-identified muons is different from that of true photons

Table 1: Background targeted by all BDTs used in this analysis, together with key properties in use that discriminates signal from backgrounds.

There are 5 BDTs utilized to target 4 types of backgrounds. The goal of each BDT together with the training signals are summarized in Tab. 1. It is worth noting that the Second Shower Veto (SSV) BDT is not trained on an event-by-event level; instead, it's trained and tested with clusters, of which there might be many in any one event. Thus, for each event, the output of the SSV is a vector of BDT scores for all candidate second-shower clusters. Also worth noting is that we do not directly cut on the SSV BDT, but instead feed the output of the SSV BDT as training variables into the NC $1\pi^0$ BDT.

Figure 3 shows stacked BDT response distributions of signal and background for all 5 BDTs after the pre-selection stage.

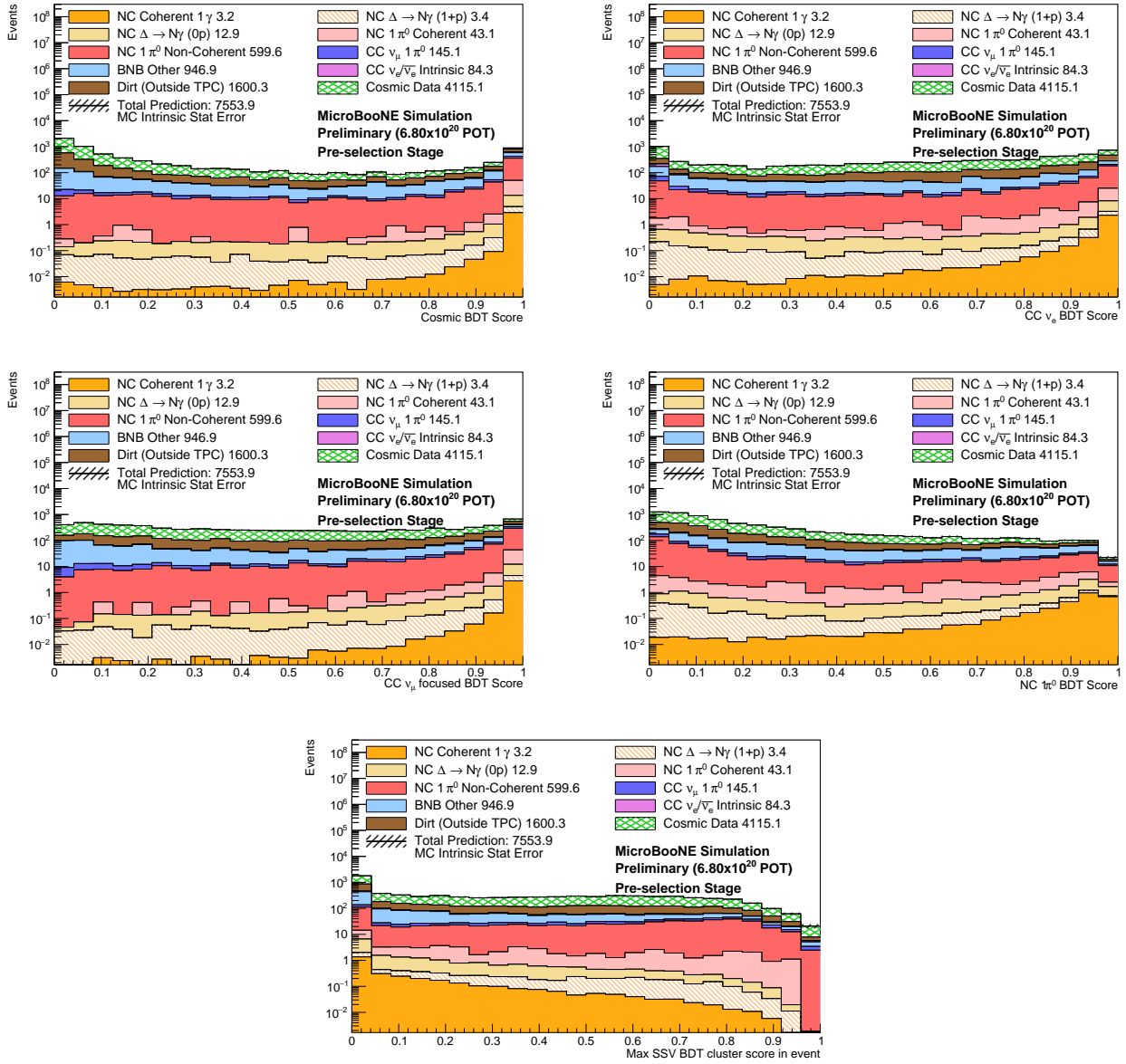


Figure 3: BDT distributions for the 5 BDTs used in this analysis. By construction BDT scores are in the range $[0,1]$. Events with a higher BDT score are more likely to be NC coherent 1γ events except for the SSV BDT, where a higher SSV BDT score indicates that the second shower candidate is more likely coming from a π^0 decay.

2.4 Preliminary Results on Simulation

We apply cuts on the Cosmic, CC ν_e , CC ν_μ and NC π^0 BDTs and refer to the resulting selection as the “final selection”. The cut positions of the BDTs are optimized towards the maximum statistical-only significance of the signal NC 1γ coherent sample, $N_{\text{sig}}/\sqrt{N_{\text{bkg}}}$, for MicroBooNE Runs 1-3.

The selection efficiency at final selection for the signal NC 1γ coherent sample is 12.5% relative to all simulated events in the active TPC. The final efficiencies for all signal and background categories are shown in Tab. 2, calculated relative to the topological selection stage. The final selection achieves a 95.3% rejection of non-coherent NC π^0 and a 99.97% rejection of cosmic events, while keeping signal efficiency high as 44.7%. Figure 4 shows the final selection efficiency for NC coherent 1γ signal as a function of key variables: the true photon energy and the true photon angle $\cos(\theta)$ respectively.

Category	Pre-Selection Eff	Final Eff.
NC Coherent 1γ	97.03 %	44.71 %
NC $\Delta \rightarrow N\gamma$ (0p)	96.73 %	18.88 %
NC $\Delta \rightarrow N\gamma$ (1+p)	95.58 %	7.87 %
NC $1\pi^0$ Coherent	95.36 %	8.24 %
NC $1\pi^0$ Non-Coherent	94.85 %	4.68 %
CC $\nu_\mu 1\pi^0$	88.77 %	3.02 %
BNB Other	80.86 %	0.30 %
CC $\nu_e/\bar{\nu}_e$ Intrinsic	93.08 %	0.68 %
Dirt (Outside TPC)	60.69 %	0.24 %
Cosmic Data	60.05 %	0.03 %

Table 2: Efficiencies for all signal and background categories at the pre-selection stage and final selection stage, relative to the number of events at the topological selection stage.

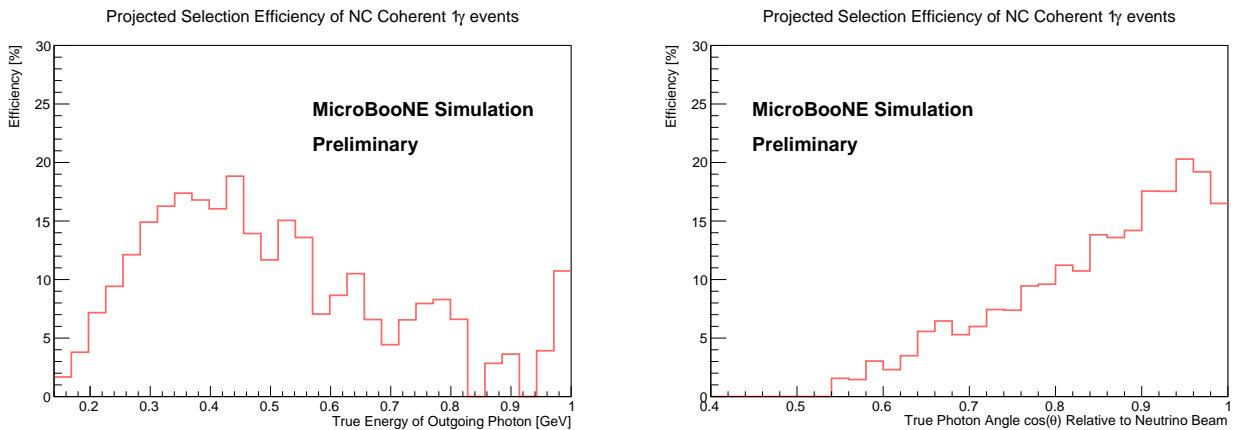


Figure 4: Final selection efficiency for the signal NC 1γ coherent sample as a function of true photon energy (left) and true photon angle with respect to the beam (right). Selection efficiency for photons with angle $\cos(\theta) < 0.4$ is 0% thus in this plot we only show selection efficiency for forward-going photons with $\cos(\theta) > 0.4$.

Figure 5 shows distributions of reconstructed quantities of the two key variables in the final selection: (a) reconstructed shower energy, (b) reconstructed shower $\cos\theta$.

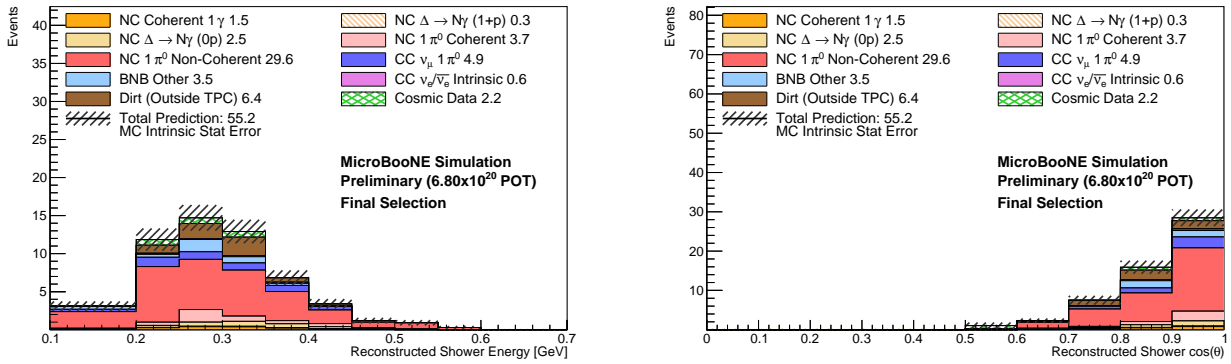


Figure 5: Two distributions of interest in the final selection showing the phase space for the reconstructed shower energy (left), the reconstructed shower angle w.r.t the beam (right).

2.5 Potential Future Improvements

A key characteristic for coherent (or “coherent-like”) event is lack of hadrons in the interaction final state. However it’s found that the final selection still sees a non-negligible amount of events with protons exiting the nucleus. For the dominant NC $1\pi^0$ non-coherent background, 49.4% of selected NC $1\pi^0$ non-coherent events have protons exiting the nucleus. A new tool, called proton stub veto (PSV) BDT is developed to reduce this background. The goal of the PSV is to reject neutrino interactions with protons exiting the nucleus in the final state, and a cut on the PSV can be applied after the final selection to yield a more “coherent-like” selection.

The PSV achieves its goal by identifying any candidate proton track in the event. Two key properties of protons are used: first, protons originating from the neutrino interaction should intersect the backward projection of the reconstructed shower direction at the true interaction vertex; second, the proton track has Bragg peak at the end. Like the second shower veto BDT, the PSV BDT is also trained and tested with clusters, and its output is a vector of BDT scores for all candidate proton clusters in one event. While the ultimate goal is to reject events with protons exiting the nucleus using an event-level metric, studies are still underway to optimize choice of this metric to maximize the BDT’s rejection power. In this note, we show examples of how the maximum PSV BDT score among all candidate clusters in one event may be used as an event-level metric. A future performance improvement is expected with optimization of the PSV cut, simultaneously with the other cuts, or independently.

Figure 6 is an example demonstrating the preliminary projected efficiency of the PSV BDT in rejecting NC non-coherent $1\pi^0$ backgrounds. As seen in right plot of Fig. 6, an arbitrarily chosen cut at 0.5 on the maximum PSV BDT score yields a peak rejection efficiency of 65% for NC non-coherent $1\pi^0$; moreover, it rejects events with exiting proton KE less than 10 MeV at efficiency of $\sim 20\%$, and events with exiting proton KE between ~ 10 -20 MeV at efficiency $>50\%$. Efficiencies are calculated with respect to topological selection stage.

In Fig. 7 we show the stacked BDT response distribution of signal and background for the PSV after the pre-selection stage on the left, and the maximum PSV BDT score distribution after the final selection on the right.

We observe that in the final selection there are events with both low PSV score (corresponding to events that look truly coherent) and events with high PSV scores (indicating evidence of some hadronic activity in the back-projection of the shower). We highlight three selected data events corresponding to both high and low PSV score:

- Run: 5385, SubRun: 23, Event: 1171: Fig. 8 highlights an event that according to primary Pandora reconstruction information is a single shower, but a high proton veto score is indicative of a missing proton stub.

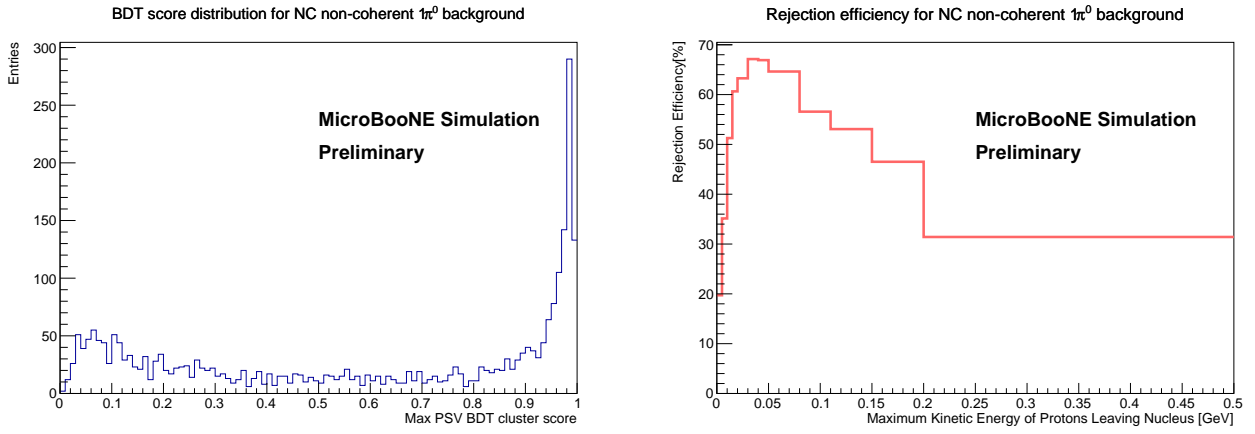


Figure 6: An example showing potential power of the PSV BDT in rejecting NC non-coherent $1\pi^0$ backgrounds. Left: max PSV scores of all candidate clusters in true NC non-coherent $1\pi^0$ events inside the active TPC after the topological stage. Right: NC non-coherent $1\pi^0$ rejection efficiency if a cut at 0.5 on maximum PSV score is placed, shown as a function of maximum kinetic energy of protons exiting the nucleus in the event. Efficiency is calculated relative to true NC non-coherent $1\pi^0$ events included in the left plot. For the sake of study PSV BDT efficiency, no pre-selection cuts and other BDT cuts are applied.

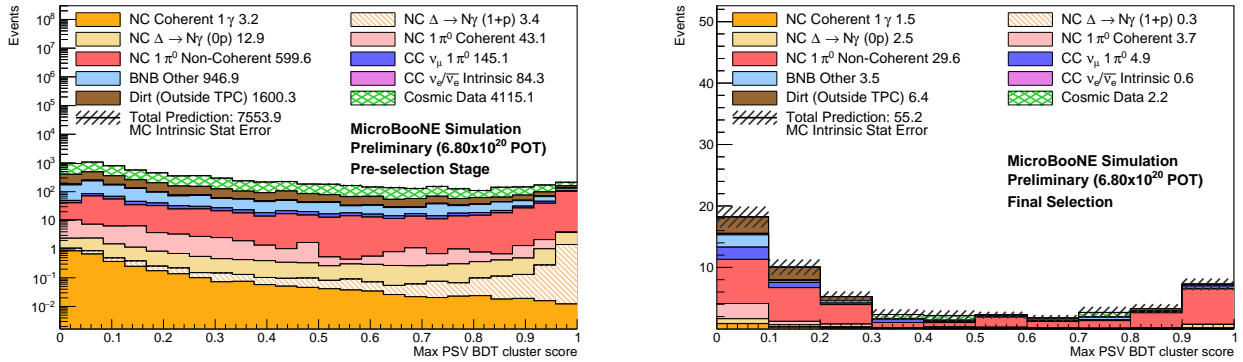


Figure 7: BDT distributions for PSV BDT after the pre-selection stage (left) and the final selection stage (right). Note that the left plot is in logarithmic scale while the right in linear scale. By construction BDT scores are in the range $[0,1]$. A high score indicates a higher likelihood of a proton stub in the event.

- Run: 5519, SubRun: 99, Event: 5000: Fig. 9 shows a single shower event with very low proton veto score.
- Run: 5643, SubRun: 54, Event: 2712: Fig. 10 highlights the second shower veto. Where as the previous two event displays have a low second shower veto score, indicating a lower probability of a second shower being present, this event scores high and is consistent with a visible second shower candidate.

While the cut value for PSV BDT has not yet been optimized, we can investigate the performance of PSV BDT orthogonal to other BDTs used in the analysis. The right plot in Fig. 11 shows the reconstructed shower energy distribution if an additional cut on maximum PSV BDT score is placed on events passing the final selection at 0.5 (value picked by eye). This indicates that additional 41% of the NC non-coherent π^0 background can be further rejected while only $\sim 14\%$ of the signal is lost, highlighting the potential of an orthogonal PSV cut.

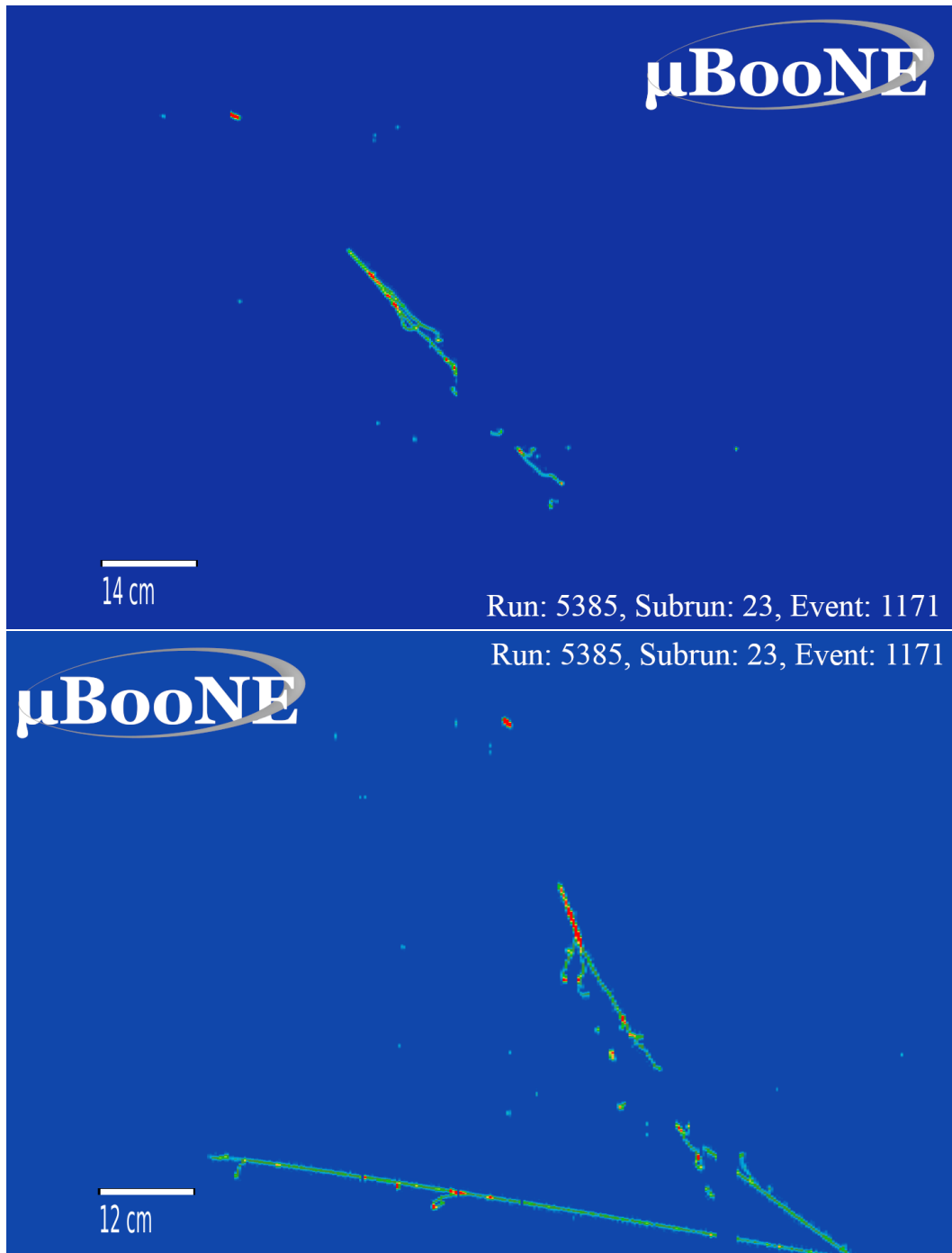


Figure 8: Data event, Run: 5385 SubRun: 23 Event 1171. This single shower event is reconstructed as a 237.3 MeV shower. It has a max proton veto score on plane 2 and plane 1 of 0.988 and 0.904 respectively indicating a high likelihood of a proton stub in the backward vicinity of the shower. Shown above is the event display for plane 2 (top) and plane 1 (bottom) showing a clean single shower and what looks like a highly ionizing proton stub consistent with the PSV scores assigned. It has a low SSV score indicating no evidence of a secondary shower.

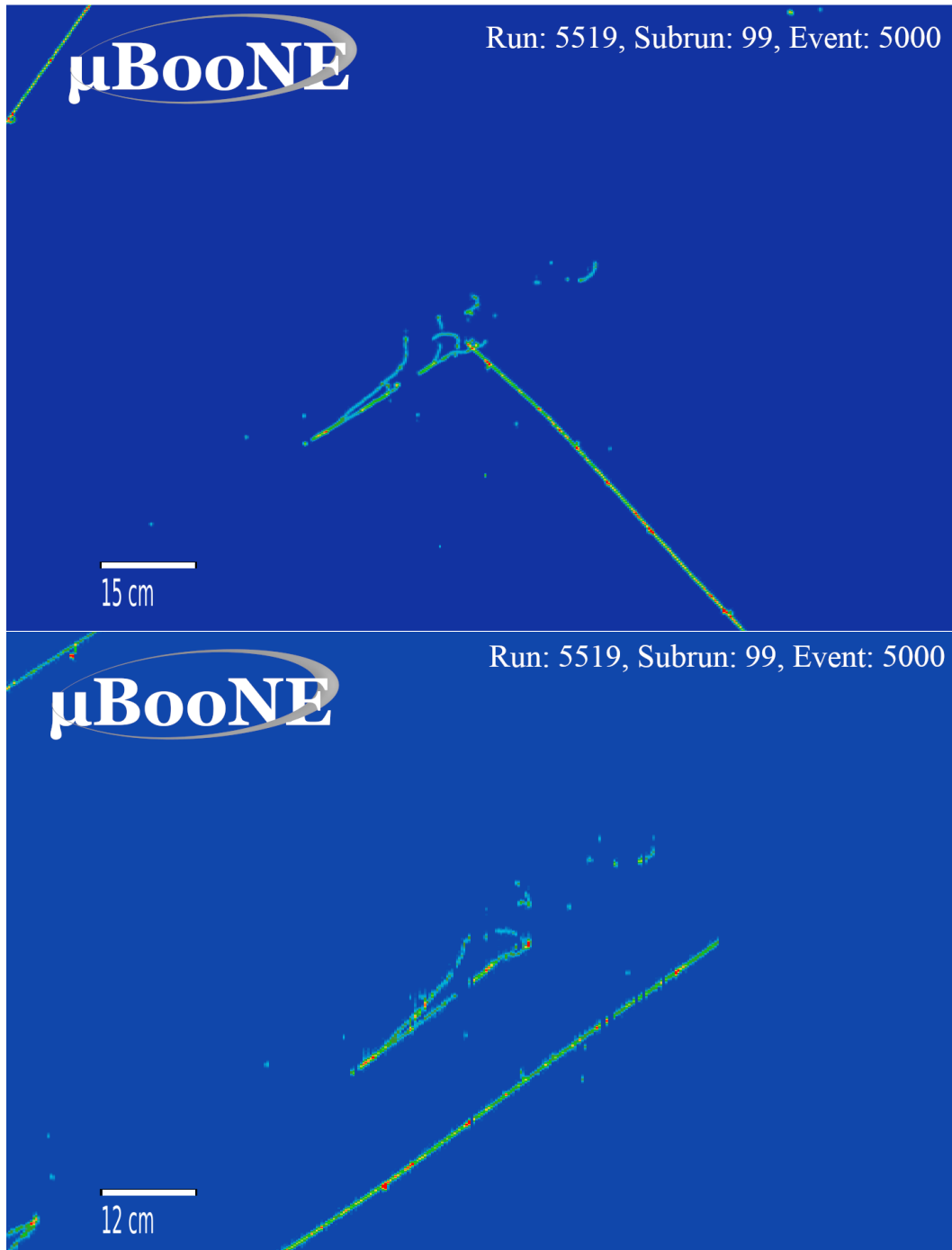


Figure 9: Data event, Run: 5519 SubRun: 99 Event 5000. This single shower event is reconstructed as a 209.0 MeV shower. It has a low max proton veto score on plane 2 and plane 1 of 0.028 and 0.015 respectively indicating a low likelihood of a proton stub in the backward vicinity of the shower. Shown above is the event display for plane 2 (top) and plane 1 (bottom) showing a clean single shower. There is a very small bit of activity behind the shower although this was included in the primary shower by Pandora. It has a low SSV score indicating no evidence of a secondary shower.

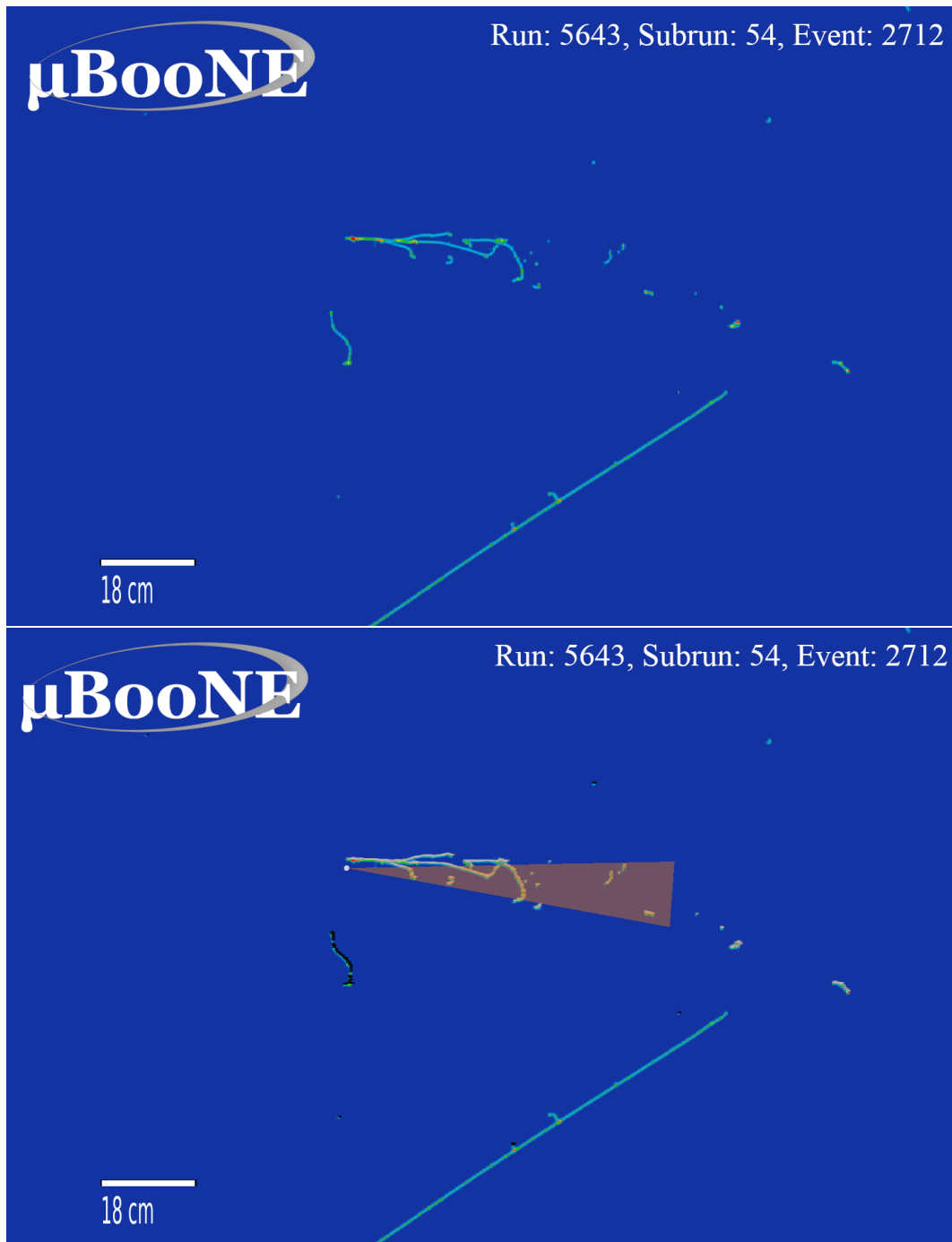


Figure 10: Data event, Run: 5643 SubRun: 54 Event 2712. This single shower event is reconstructed as a 251.2 MeV shower. It has a low max proton veto score on plane 2 and plane 1 of 0.059 and 0.056 respectively indicating a low likelihood of a proton stub in the backward vicinity of the shower. There was a high SSV score indicating a high likelihood of a secondary shower. Shown above is the event display for plane 2 both with (top) and without (bottom) the information of Pandora reconstructed objects drawn. There is a clear primary shower, and what looks like a missed secondary shower highlighted in black, which indicates they are in the slice as unassociated hits (the objects that make up the SSV candidate clusters).

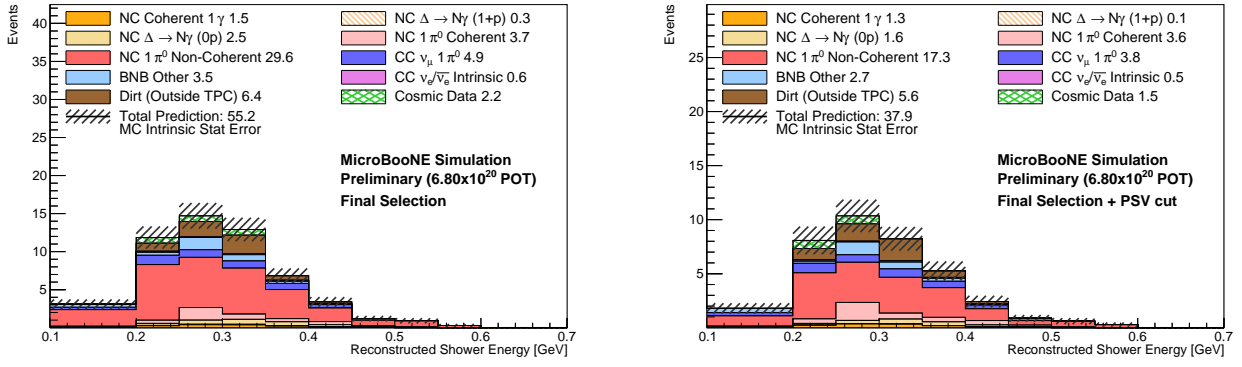


Figure 11: Reconstructed shower energy distribution in the final selection (left) and after additional cut of 0.5 on max PSV cluster score following the final selection (right).

3 Summary

We have presented a search for NC coherent-like single photon events with MicroBooNE Run 1-3 Monte Carlo. This analysis has yielded 95% rejection efficiency for the dominant source of background to single-photon searches (NC non-coherent π^0 background), and 99.9% rejection efficiency for cosmic background, at final selection. The presented work also shows the excellent potential of a newly developed proton-veto tool in further removal of background with hadronic activity. Validation is being carried out with the open data sets before we proceed with unblinding the main data set.

References

- [1] R. Acciarri *et al.*, “Design and Construction of the MicroBooNE Detector,” *JINST*, vol. 12, no. 02, p. P02017, 2017.
- [2] A. A. Aguilar-Arevalo *et al.*, “Significant Excess of ElectronLike Events in the MiniBooNE Short-Baseline Neutrino Experiment,” *Phys. Rev. Lett.*, vol. 121, no. 22, p. 221801, 2018.
- [3] P. Abratenko *et al.*, “Search for neutrino-induced neutral-current Δ radiative decay in microboone and a first test of the miniboone low energy excess under a single-photon hypothesis,” *Phys. Rev. Lett.*, vol. 128, p. 111801, Mar 2022.
- [4] A. A. Aguilar-Arevalo *et al.*, “Updated miniboone neutrino oscillation results with increased data and new background studies,” *Phys. Rev. D*, vol. 103, p. 052002, Mar 2021.
- [5] E. Wang, L. Alvarez-Ruso, and J. Nieves, “Photon emission in neutral-current interactions at intermediate energies,” *Phys. Rev. C*, vol. 89, p. 015503, Jan 2014.
- [6] P. Ballett, S. Pascoli, and M. Ross-Lonergan, “ $u(1)'$ mediated decays of heavy sterile neutrinos in miniboone,” *Phys. Rev. D*, vol. 99, p. 071701, Apr 2019.
- [7] P. Ballett, M. Hostert, and S. Pascoli, “Dark neutrinos and a three-portal connection to the standard model,” *Phys. Rev. D*, vol. 101, p. 115025, Jun 2020.
- [8] C. A. Argüelles, M. Hostert, and Y.-D. Tsai, “Testing new physics explanations of the miniboone anomaly at neutrino scattering experiments,” *Phys. Rev. Lett.*, vol. 123, p. 261801, Dec 2019.
- [9] E. Bertuzzo, S. Jana, P. A. N. Machado, and R. Zukanovich Funchal, “Dark neutrino portal to explain miniboone excess,” *Phys. Rev. Lett.*, vol. 121, p. 241801, Dec 2018.
- [10] R. Acciarri *et al.*, “The pandora multi-algorithm approach to automated pattern recognition of cosmic-ray muon and neutrino events in the microboone detector,” *The European Physical Journal C*, vol. 78, no. 1, p. 82, 2018.
- [11] A. A. Aguilar-Arevalo *et al.*, “Search for electron neutrino appearance at the $\Delta m^2 \sim 1 \text{ eV}^2$ scale,” *Phys. Rev. Lett.*, vol. 98, p. 231801, Jun 2007.
- [12] P. Abratenko *et al.*, “New CC0 π genie model tune for microboone,” *Phys. Rev. D*, vol. 105, p. 072001, Apr 2022.
- [13] C. Andreopoulos *et al.*, “The GENIE Neutrino Monte Carlo Generator,” *Nucl. Instr. and Meth. A*, vol. 614, pp. 87–104, 2010.
- [14] J. Tena-Vidal *et al.*, “Neutrino-nucleon cross-section model tuning in GENIE v3,” *Phys. Rev. D*, vol. 104, no. 7, p. 072009, 2021.
- [15] “Measurement of space charge effects in the MicroBooNE LArTPC using cosmic muons,” *Journal of Instrumentation*, vol. 15, pp. P12037–P12037, dec 2020.
- [16] T. Chen and C. Guestrin, “XGBoost: A Scalable Tree Boosting System,” *arXiv e-prints*, p. arXiv:1603.02754, Mar. 2016.